Am J Transl Res 2016;8(1):188-195
www.ajtr.org /ISSN:1943-8141/AJTR0017868

Original Article

Kisspeptin 10 inhibits the Warburg effect in breast cancer through the Smad signaling pathway: both *in vitro* and *in vivo*

Guo-Qing Song, Yi Zhao

Department of Pancreas and Breast Surgery, Shengjing Hospital of China Medical University, 36 Sanhao Street, Heping, Shenyang, Liaoning 110004, P.R. China

Received October 14, 2015; Accepted November 27, 2015; Epub January 15, 2016; Published January 30, 2016

Abstract: Breast cancer is the most frequently diagnosed cancer in females. Warburg effect could enhance tumorigenesis and has garnered attention as a target for tumor treatment. In this study, we found that the mRNA and protein levels of hexokinase 2 (HK2), pyruvate kinase (PKM2), and pyruvate dehydrogenase kinase (PDK1) in breast cancer tissues were higher than those in corresponding noncancerous tissues. HK2, PKM2, and PDK1 expression was correlated statistically with the survival rate of the patients with breast cancer. We also demonstrated a shorter fragment of KISS1, Kisspeptin-10 (KP-10), inhibited the Warburg effect and induced mitochondrial injury in human breast cancer cell line, MDA-MB-231. We confirmed that KP-10-inhibited the Warburg effect by activating Smad pathway. The effects and related mechanisms of these treatments were also confirmed in murine xenografts. However, additional studies are needed to confirm these results in other cell types.

Keywords: Kisspeptin-10, Warburg effect, mitochondrial injury, Smad pathway, murine xenografts

Introduction

Breast cancer is the most common malignancy and the leading cause of cancer-related mortality among women in the world [1]. Human breast tumorigenesis is thought to require multiple gene mutations, and different tumors often have distinct molecular abnormalities [2].

KISS1 was initially discovered by Lee et al. [3] in experiments designed to identify the molecules responsible for the antimetastatic effect of human chromosome 6. *KISS1* encodes a 145-amino acid protein, being processed into kisspeptins of several sizes [4, 5]. Associations between KISS1 expression loss and increased tumor progression and poor prognosis were found in several solid tumors, such as colorectal cancer, lung cancer, and breast cancer [6-8]. Previous studies have shown the mechanisms of KISS1. For example, metastin (encoded from the KISS1 gene) induces Ca^{2+} in receptor-transfected Chinese hamster ovary (CHO) cells, as well as phosphorylation of ERK1/2 and weak phosphorylation of p38/MAPK but not of SAPK/JNK3 [9]. To our knowledge, no previous studies showed the relationship between Kisspeptin-10 (KP-10) and the Warburg effect in breast cancer cells.

The Warburg effect, also known as aerobic glycolysis, is a shift from oxidative phosphorylation to glycolysis, and is considered to be the root of cancer development and progression [10]. We carried out this experiment to better understand and confirm if KP-10 could inhibit the Warburg effect in breast cancer cells.

Materials and methods

Patients

This study was approved by Our University Ethics Committee and was conducted in accordance with the Helsinki Declaration. Written informed consent for participation in the study was obtained from participants. A total of 28 patients with breast cancer was obtained from the Department of Pancreas and Breast Surgery, Shengjing Hospital of China Medical

University. None of the patients underwent radiotherapy or chemotherapy before the operation.

Real-time PCR

Total RNA was isolated from tissues using an RNeasy Mini Kit (Biomed, Beijing, China). First strand cDNA was reverse transcribed with 1 μg of total RNA, using TaKaRa Reverse Transcription Kit (TaKaRa, Dalian, China) and oligo (dT) 15 primers (TaKaRa). The resultant cDNA was then used for quantitative PCR reactions. The *hexokinase 2 (HK2)* primers were: sense-5'-ATTGTCCAGTGCATCGCGGA-3' and antisense-5'-AGGTCAAACTCCTCTCGCCG-3'. The *pyruvate kinase 2 (PKM2)* primers were: sense-5'-GTCGAAGCCCCATAGTGAAG-3' and antisense-5'-GTGAATCAATGTCCAGGCGG-3'. The *pyruvate dehydrogenase kinase 1 (PDK1)* primers were: sense-5'-ATTCAAGTTCATGTCACGCTGG-3' and antisense-5'-TTTCCTCAAAGGAACGCCAC-3'. *GAPDH* was used as internal controls for normalization of the results. The *GAPDH* primers were: sense-5'-AGAAGGCTGGGGCTCATTTG-3' and antisense-5'-AGGGGCCATCCACAGTCTTC-3'. Amplification was performed with 1 cycle at 95°C for 10 min, and 40 cycles of 95°C for 15 s and 60°C for 60 s. Calculation of the relative expression of each transcript was performed using the $2^{-\Delta\Delta Ct}$ method.

Cell culture and treatment

MDA-MB-231 cell line was purchased from the American Type Culture Collection (Rockville, MD, USA) and maintained in DMEM supplemented with 10% FCS and antibiotics (100 μM penicillin and 100 μM streptomycin). Cells were maintained in a humidified cell incubator with 5% CO_2 at 37°C. Then the cells were treated with 62.5 nM KP-10 (Abcam, Cambridge, UK) for 24 hours at 37°C (11).

Plasmid and transfection

MDA-MB-231 cells were seeded in 10-cm dishes and grown overnight to 70% confluency, trypsinized and transfected with *Smad2* shRNA plasmid (sc-38374-SH, Santa Cruz biotechnology, Santa Cruz, CA, USA) using Lipofectamine™ 2000 (Invitrogen, Carlsbad, CA, USA) according to the manufacturer's instructions.

Determination of mitochondrial membrane potential

Mitochondrial membrane potential (MMP) was analyzed using the fluorescent dye 5,5',6,6'-tetrachloro-1,1',3,3'-tetraethylbenzimidazolycarbocyanine iodide (JC-1) following the manufacturer's protocol (KeyGEN, Nanjing, China). Briefly, cells were plated in 6-well culture plate. After treatment for 24 h, cells were washed twice with PBS, harvested and incubated with 20 nM JC-1 for 30 min in the dark. MMP was then analyzed both using a FACS Calibur machine (Model FACSC 420, Baltimore, MD, USA) and an Olympus CX71 fluorescence microscope (Olympus, Tokyo, Japan).

LDH activity, lactate production, and glucose utilization assay

Cells (1×10^6) were prepared for LDH activity and lactate production assay using a Lactate Dehydrogenase Activity Assay Kit and Lactate Assay Kit (Sigma Chemicals, St Louis, MO, USA) according to the manufacturer's protocol. For glucose utilization assay, cells were incubated for 24 hours. The culture media were replaced with phenol-red free RPMI with 1% FBS in continuous culture for 3 days. Medium specimens were collected each day. Glucose concentrations in the media were measured using a colorimetric glucose assay kit (BioVision, Milpitas, CA, USA) and normalized according to cell number.

Western blot analysis

Proteins were resolved by 10% SDS-PAGE, transferred to a nitrocellulose membrane, and detected using the following antibodies: HK2 (2016, Cell Signaling Technology, Danvers, MA, USA), PKM2 (3198, Cell Signaling Technology), PDK1 (3062, Cell Signaling Technology), P-Smad3 (sc-130218, Santa Cruz), Smad3 (sc-101154, Santa Cruz), P-Smad2 (sc-135644, Santa Cruz), Smad2 (sc-6200, Santa Cruz), Bcl-xL (sc-8392, Santa Cruz), Bcl-2 (sc-783, Santa Cruz), Bad (sc-8044, Santa Cruz), Bak (sc-7873, Santa Cruz), Bax (sc-7480, Santa Cruz), caspase 3 (sc-7272, Santa Cruz), caspase 9 (sc-7885, Santa Cruz), and β-actin (sc-47778, Santa Cruz). Immunostaining was detected using an enhanced chemiluminescence (ECL) system (Amersham Biosciences, Westborough, MA, USA).

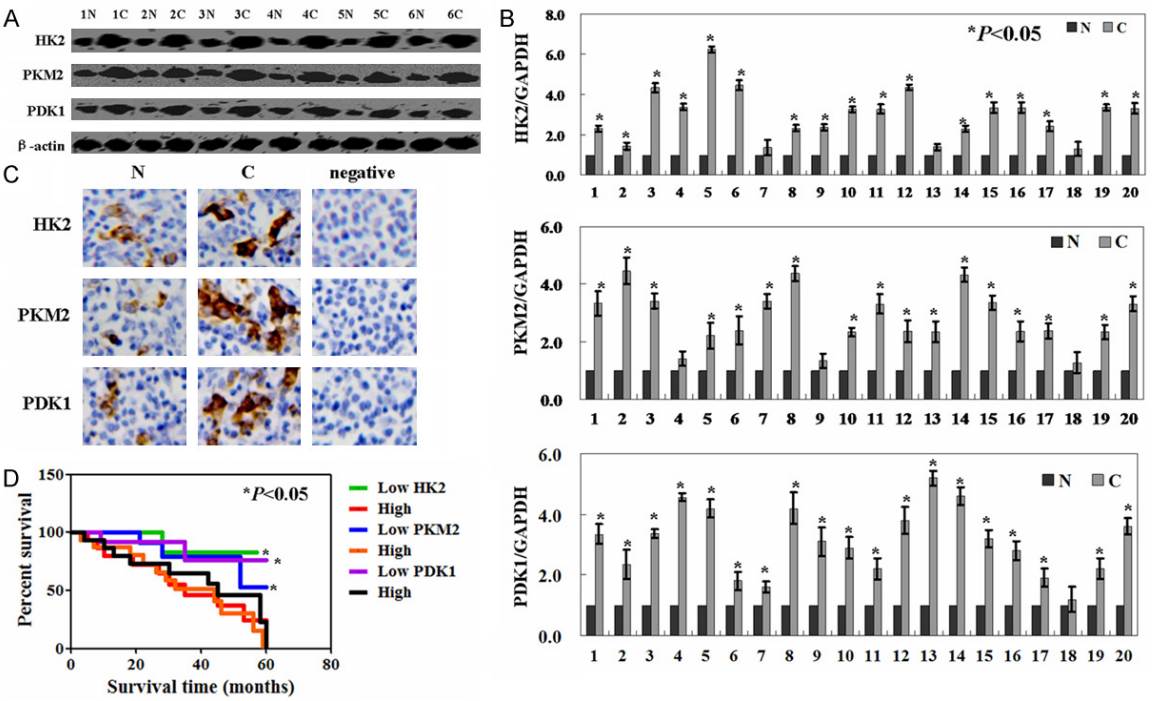

Figure 1. HK2, PKM2, and PDK1 mRNA and protein levels in breast cancer. A. Representative results of HK2, PKM2, and PDK1 expression in two paired of breast cancer tissues and corresponding normal tissue by western-blot. β-actin was used as an internal control. B. The level of *HK2*, *PKM2*, and *PDK1* mRNA was measured in specimens by using Real-time PCR. *GADPH* was used as internal controls. C. Immunohistochemical staining for HK2, PKM2, and PDK1 protein in specimens. N: Normal, C: Cancer. D. Kaplan-Meier curves for cumulative survival rate of the patients with breast cancer according to the HK2, PKM2, or PDK1 expression.

In vivo effects of KP-10 on gastric cancer xenografts

This study was approved by China Medical University Ethics Committee. NOD SCID mice (4 to 6-weeks-old, Charles River, Wilmington, MA, USA) were injected subcutaneously with MDA-MB-231 cell (5×10^7 cells in 200 μL PBS) into the axilla of each mouse. The mice were examined every five day. Tumors were measured using calipers, and tumor volumes were calculated (tumor volume = length × width^2 × 0.52). The survival status of the mice was observed until the experiments were terminated.

Immunohistochemistry

Immunohistochemistry was performed on deparaffinized 5 μm sections. Paraffin sections were stained with the first antibody as described in Western blot by incubating overnight at 4°C. Secondary staining with biotinylated secondary antibodies and tertiary staining with a streptavidin horseradish peroxidase (HRP) complex (Beyotime, Beijing, China) were performed for 60 min at room temperature. Then, the sections were counterstained with hematoxylin (Beyotime).

Statistical analysis

Data are presented as the mean ± standard deviation (SD). Differences between groups were analyzed using Student's t-test. Statistical analysis was performed using the Statistical Package for the Social Sciences (SPSS, version 17.0; SPSS, Inc.) and significance was established at $P<0.05$.

Results

HK2, PKM2, and PDK1 were down-regulated in breast cancer tissues compared with normal tissues

In **Figure 1A** and **1B**, the levels of HK2, PKM2, and PDK1 mRNA and protein in breast cancer tissues were significantly higher than those in corresponding adjacent noncancerous tissue. The results of immunohistochemical staining

Table 1. Relationship between HK2, PKM2, and PDK1 expression and clinicopathological parameters of patients with breast cancer

Clinicopathological features		HK2				PKM2				PDK1			
	n	Low	High	χ^2	P	Low	High	χ^2	P	Low	High	χ^2	P
Median age (range)	54 years (38-71 years)												
Median tumor size (range)	27 mm (6-65 mm)												
Histology				2.157	0.340			0.469	0.7909			4.279	0.1177
Invasive ductal carcinoma	10	2	8			4	6			6	4		
Invasive lobular carcinoma	12	6	6			4	8			4	8		
Medullary carcinoma	6	2	4			3	3			5	1		
Stage				0.052	0.974			0.574	0.7505			1.197	0.5498
1	8	3	5			3	5			3	5		
2A	8	3	5			4	4			5	3		
2B	12	4	8			4	8			7	5		
Grade				2.813	0.245			4.578	0.1045			0.562	0.7550
1	11	6	5			7	4			5	6		
2	8	2	6			2	6			5	3		
3	9	2	7			2	7			5	4		
Lymph node status				0.029	0.864			0.377	0.539			0.673	0.4120
-	12	4	8			6	6			8	4		
+	16	6	10			5	11			7	9		
Recurrence status				5.324	0.02			13.93	0.0002			7.269	0.007
-	8	6	2			8	0			8	0		
+	20	4	16			3	17			7	13		

Abbreviations: PR positive rate, χ^2 Chi-square distribution.

showed that positive staining was seen in the cytoplasm of the cancer cells, in contrast, almost no positive cells were seen in normal tissues (**Figure 1C**). Furthermore, we found that the HK2, PKM2, and PDK1 expression was correlated with the recurrence of breast cancer (**Table 1**, $P < 0.05$). Breast cancer patients with HK2, PKM2, or PDK1 expression were associated with a lower survival rate than the ones without HK2, PKM2, or PDK1 expression (**Figure 1D**, $P < 0.05$).

The effects of KP-10 on the Warburg effect in breast cancer cells

Immunofluorescence analysis showed the changes of MMP in breast cancer cells with KP-10 treatment (**Figure 2A**). Quantitative results were calculated by using flow cytometry, which showed that the ratio of red/green was reversed in breast cancer cells after KP-10 treatment (**Figure 2B**). To determine whether KP-10 treatment exerts any effects on Warburg effect in breast cancer cells, glucose uptake, LDH activity, and oxygen consumption were determined. Oxygen consumption was increased in breast cancer cells by KP-10 treatment (**Figure 2D**, $P < 0.05$), while glucose uptake, lactate production, and LDH activity was decreased in KP-10 treated ones (**Figure 2C**, **2E** and **2F**, $P < 0.05$). Furthermore, in the aspect of pyruvate, the cytoplasmic pyruvate level was decreased in KP-10 treated cells (**Figure 2G**, $P < 0.05$). Interestingly, the effects of KP-10 on the Warburg effect in breast cancer cells were offset by using *Smad2* shRNA (**Figure 2**, $P < 0.05$). These results indicated that KP-10 may play its effects in breast cancer cells through the Smad signaling pathway.

KP-10 activated the Smad signaling pathway in breast cancer cells

Western blot analysis showed that the levels of HK2, PKM2, and PDK1 protein were significantly decreased in breast cancer cells after KP-10 treatment (**Figure 3**, left panel). Furthermore, we found that phosphorylated levels of Smad2 and Smad3 significantly increased in breast cancer cells with KP-10 treatment (**Figure 3**, left panel), while total protein levels of Smad2 and Smad3 remained unchanged (**Figure 3**, left panel). The results above showed that the changes of mitochondria in breast cancer cells

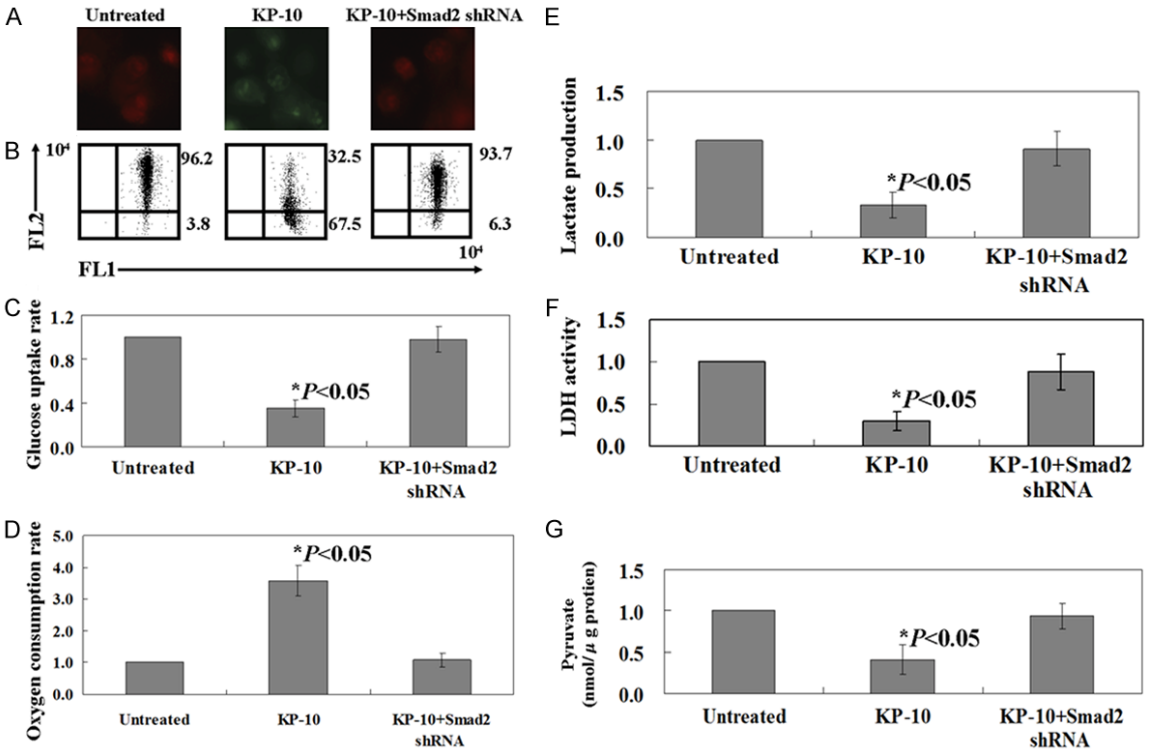

Figure 2. KP-10 reversed Warburg effect in breast cancer cells. Mitochondrial-Membrane Potential (Δψ*m*) was analyzed by immunofluorescence (A) and flow cytometry (B). (C) Glucose uptake, (D) Oxygen consumption, (E) LDH activity, (F) Lactate production and (G). Cytoplasmic pyruvate were detected in breast cancer cells. Untreated: Untreated MDA-MB-231 cells; KP-10: MDA-MB-231 cells treated with KP-10; KP-10+*Smad2* shRNA: MDA-MB-231 cells treated with KP-10 and transfected with *Smad2* shRNA.

with KP-10 treatment. As shown in **Figure 3** (right panel), we found that a decrease in Bcl-2 and Bcl-xL expression and an increase in Bax, Bad, and Bak expression in breast cancer cells with KP-10 treatment. After KP-10 treatment, caspase 9 and caspase 3 was significantly increased in breast cancer cells (**Figure 3**, right panel). We used β-actin as an internal control in the entire process.

KP-10 inhibited tumor growth in vivo

We next determined whether KP-10 displays anti-tumor properties in established xenograft tumor models. Macroscopic appearance of subcutaneous tumors was shown in **Figure 4A**. Furthermore, we also found liver metastases in the mice without KP-10 treatment and the mice with both KP-10 and *Smad2* shRNA treatment (**Figure 4B**). KP-10 resulted in a significantly reduced tumor size in nude mice (**Figure 4C**, $P < 0.05$). We also found that the KP-10-treated group had a better survival rate compared to that of the untreated mice, and both KP-10 and *Smad2* shRNA treated groups (**Figure 4D**, $P < 0.05$). The results of immunohistochemistry showed that the levels of P-Smad2, P-Smad3, Bax and Bad significantly increased with KP-10 treatment in both *in situ* tumor and metastatic tumor (**Figure 4E** and **4F**).

Discussion

The Warburg effect is proven to enhance tumorigenesis and has garnered attention as a target for tumor treatment [12, 13]. In this study, we found that the HK2, PKM2, and PDK1 expression was correlated statistically with the recurrence of breast cancer. Liu et al. [14] reported that the KISS1 inhibits aerobic glycolysis and increases oxidative phosphorylation, strongly suggesting that aerobic glycolysis it may contribute to successful metastasis. In our previous studies, we have found that KP-10 inhibits the migration of breast cancer cells [11]. In this study, we found that KP-10 could inhibit the Warburg effect in breast cancer cells. These results indicated that Warburg effect is related to tumor metastasis.

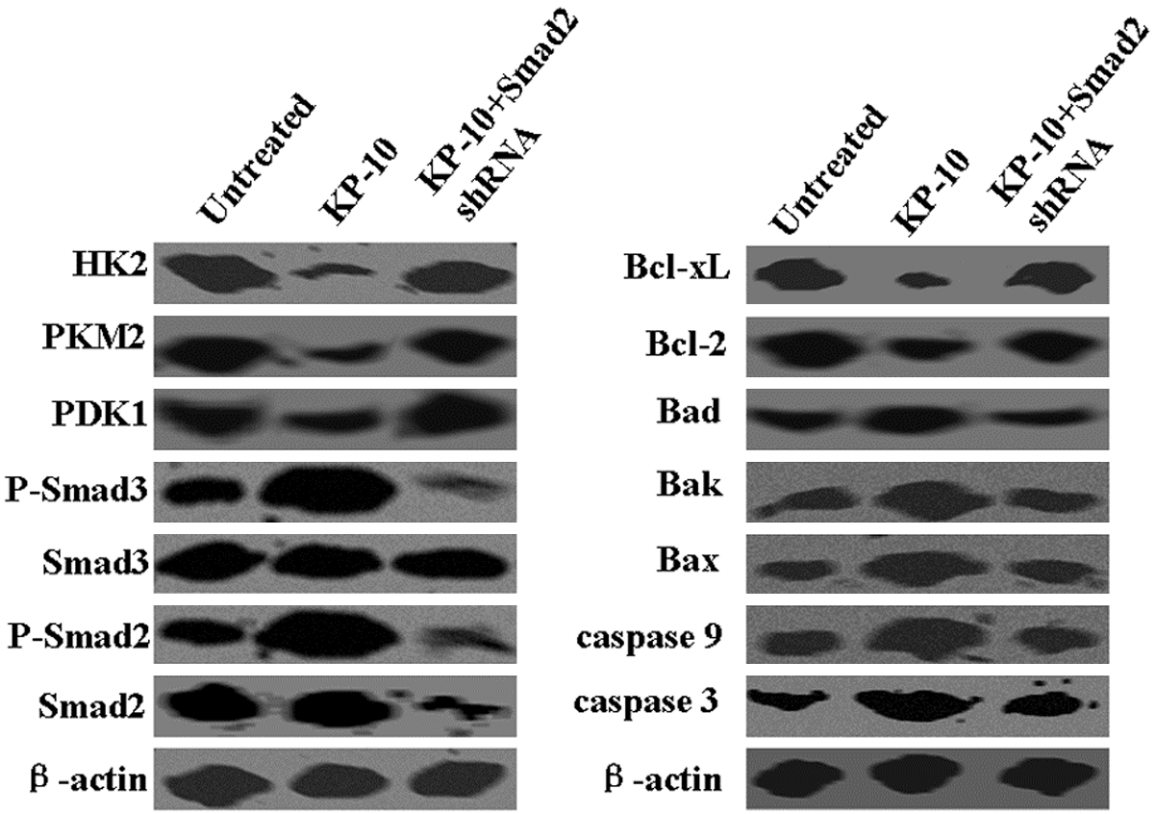

Figure 3. The potential mechanisms of KP-10 suppressed Warburg effect. Cell lysates were electrophoresed and HK2, PKM2, PDK1, P-Smad3, Smad3, P-Smad2, Smad2, Bcl-xL, Bcl-2, Bad, Bak, Bax, caspase 3, and caspase 9 proteins were detected by their specific antibodies. Untreated: Untreated MDA-MB-231 cells; KP-10: MDA-MB-231 cells treated with KP-10; KP-10+*Smad2* shRNA: MDA-MB-231 cells treated with KP-10 and transfected with *Smad2* shRNA.

Furthermore, we found that KP-10 could activate the Smad signaling pathway in breast cancer cells. According to the specific functions, Smads can be classified into the receptor-regulated Smads (R-Smads: Smad1, 2, 3, 5 and 8), inhibitory Smads (anti-Smads: Smad6 and 7), and the common mediator Smads (Co-Smads: Smad4) [15]. Xia et al. [16] found crizotinib-activated Smad signaling pathway could induce apoptosis in Lewis lung carcinoma cells. Tang et al. [17] also found that CSMD1 exhibits antitumor activity in A375 melanoma cells through activation of the Smad pathway. Smad pathway-mediated apoptosis involves activation of caspase proteases, enhanced generation of reactive oxygen species (ROS), loss of mitochondrial membrane potential and alterations in expression of the Bcl-2 family of proteins [18]. Consistent with previous studies, we also found mitochondrial injury in breast cells with activation of Smad pathway. In addition, a decrease in Bcl-2 and Bcl-xL expression and an increase in Bax, Bad, and Bak expression also were observed in breast cancer cells with KP-10 treatment.

Conclusion

To sum up, our results suggest that HK2, PKM2, and PDK1 expression was correlated with the prognosis of the patients with breast cancer. KP-10 inhibits the Warburg effect and induces mitochondrial injury in breast cancer cells. These effects may be linked to activation of the Smad signaling pathway. Our findings will need to be validated in other cancer cell lines in future.

Acknowledgements

We are indebted to Liu Xiao for his helpful criticism of the manuscript and excellent technical assistance.

Disclosure of conflict of interest

None.

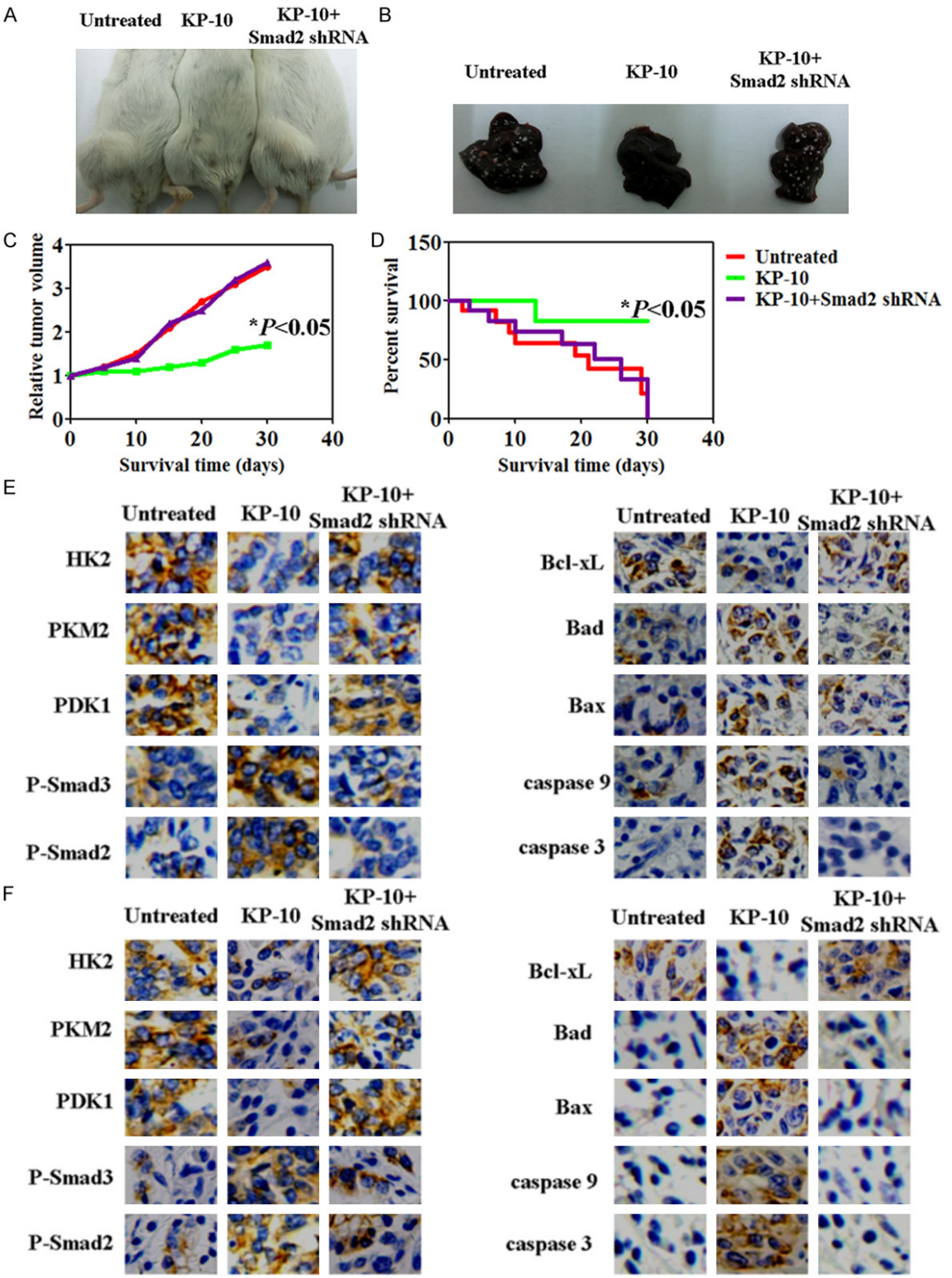

Figure 4. The role of KP-10 in xenograft mouse models. A. Macroscopic appearance of subcutaneous tumors in mice with KP-10 treatment or KP-10 and *Smad2* shRNA treatment. B. Liver metastases were found in the mice without KP-10 treatment and the mice with both KP-10 and *Smad2* shRNA treatment. C. Tumor volume of the mice with KP-10 treatment or KP-10 and *Smad2* shRNA treatment. D. Kaplan-Meier survival curves of each mice. E. Immunohistochemistry showed that the levels of P-Smad2, P-Smad3, Bax and Bad significantly increased with KP-10 treatment in *in situ* tumor. F. Immunohistochemistry showed that the levels of P-Smad2, P-Smad3, Bax and Bad significantly increased with KP-10 treatment in metastatic tumor.

Abbreviations

HK2, hexokinase 2; PKM2, pyruvate kinase; PDK1, pyruvate dehydrogenase kinase; HRP, streptavidin horseradish peroxidase; ROS, reactive oxygen species; ECL, enhanced chemiluminescence.

Address correspondence to: Dr. Yi Zhao, Department of Pancreas and Breast Surgery, Shengjing Hospital of China Medical University, 36 Sanhao Street, Heping, Shenyang, Liaoning 110004, P.R. China. E-mail: zhaozhaoyi_sj@163.com

References

[1] Kostadima L, Pentheroudakis G, Pavlidis N. The missing kiss of life: transcriptional activity of the metastasis suppressor gene KiSS1 in early breast cancer. Anticancer Res 2007; 27: 2499-2504.

[2] Visvader JE, Lindeman GJ. Transcriptional regulators in mammary gland development and cancer. Int J Biochem Cell Biol 2003; 35: 1034-1051.

[3] Lee JH, Miele ME, Hicks DJ, Phillips KK, Trent JM, Weissman BE, Welch DR. KiSS-1, a novel human malignant melanoma metastasis-suppressor gene. J Natl Cancer Inst 1996; 88: 1731-1737.

[4] Hesling C, D'Incan M, Mansard S, Franck F, Corbin-Duval A, Chèvenet C, Déchelotte P, Madelmont JC, Veyre A, Souteyrand P, Bignon YJ. In vivo and in situ modulation of the expression of genes involved in metastasis and angiogenesis in a patient treated with topical imiquimod for melanoma skin metastasis. Br J Dermatol 2004; 150: 761-767.

[5] Dhar DK, Naora H, Kubota H, Maruyama R, Yoshimura H, Tonomoto Y, Tachibana M, Ono T, Otani H, Nagasue N. Downregulation of KiSS-1 expression is responsible for tumor invasion and worse prognosis in gastric carcinoma. Int J Cancer 2004; 111: 868-872.

[6] Okugawa Y, Inoue Y, Tanaka K, Toiyama Y, Shimura T, Okigami M, Kawamoto A, Hiro J, Saigusa S, Mohri Y, Uchida K, Kusunoki M. Loss of the metastasis suppressor gene KiSS1 is associated with lymph node metastasis and poor prognosis in human colorectal cancer. Oncol Rep 2013; 30: 1449-1454.

[7] Sun YB, Xu S. Expression of KISS1 and KISS1R (GPR54) may be used as favorable prognostic markers for patients with non-small cell lung cancer. Int J Oncol 2013; 43: 521-530.

[8] Papaoiconomou E, Lymperi M, Petraki C, Philippou A, Msaouel P, Michalopoulou F, Kafiri G, Vassilakos G, Zografos G, Koutsilieris M. Kiss-1/GPR54 protein expression in breast cancer. Anticancer Res 2014; 34: 1401-1407.

[9] Lee YR, Tsunekawa K, Moon MJ, Um HN, Hwang JI, Osugi T, Otaki N, Sunakawa Y, Kim K, Vaudry H, Kwon HB, Seong JY, Tsutsui K. Molecular evolution of multiple forms of kisspeptins and GPR54 receptors in vertebrates. Endocrinology 2009; 150: 2837-2846.

[10] Garber K. Energy deregulation: licensing tumors to grow. Science 2006; 312: 1158-1159.

[11] Song GQ, Zhao Y. Kisspeptin-10 inhibits the migration of breast cancer cells by regulating epithelial-mesenchymal transition. Oncol Rep 2015; 33: 669-674.

[12] Vander Heiden MG, Cantley LC, Thompson CB. Understanding the Warburg effect: the metabolic requirements of cell proliferation. Science 2009; 324: 1029-1033.

[13] Ponisovskiy MR. Warburg effect mechanism as the target for theoretical substantiation of a new potential cancer treatment. Crit Rev Eukaryot Gene Expr 2011; 21: 13-28.

[14] Liu W, Beck BH, Vaidya KS, Nash KT, Feeley KP, Ballinger SW, Pounds KM, Denning WL, Diers AR, Landar A, Dhar A, Iwakuma T, Welch DR. Metastasis suppressor KISS1 seems to reverse the Warburg effect by enhancing mitochondrial biogenesis. Cancer Res 2014; 74: 954-963.

[15] Derynck R, Zhang Y, Feng XH. Smads: transcriptional activators of TGF-beta responses. Cell 1998; 95: 737-740.

[16] Xia P, Gou WF, Zhao S, Zheng HC. Crizotinib may be used in Lewis lung carcinoma: a novel use for crizotinib. Oncol Rep 2013; 30: 139-148.

[17] Tang MR, Wang YX, Guo S, Han SY, Wang D. CSMD1 exhibits antitumor activity in A375 melanoma cells through activation of the Smad pathway. Apoptosis 2012; 17: 927-937.

[18] Casalena G, Daehn I, Bottinger E. Transforming growth factor-β, bioenergetics, and mitochondria in renal disease. Semin Nephrol 2012; 32: 295-303.